DOI: 10.15587/978-617-8360-19-1.CH1

Anatolii Babichenko, Igor Krasnikov, Juliya Babichenko,
Oleksandr Dzevochko, Yana Kravchenko, Ihor Lysachenko

CHAPTER 1

TECHNOLOGICAL ASPECTS OF COMPUTER CONTROL OF THE SECONDARY CONDENSATION COMPLEX IN AMMONIA PRODUCTION UNDER UNCERTAINTY

ABSTRACT

The object of the study is the technological complex of secondary condensation of large-tonnage ammonia synthesis units of the AM-1360 series, which provides final cooling and separation of condensed production ammonia from circulating gas. The possibility of increasing the energy efficiency of production by modernising the equipment and technological design of the TCC has been established. This is achieved by removing the energy-intensive turbocompressor refrigeration unit (TRU) with electric drive from the circuit and creating an adaptive system of optimal software control.

The feasibility of applying a systematic approach to solving such a complex problem, based on mathematical modelling and process identification, has been demonstrated. The operating conditions of the TCSC and the primary condensation unit have been analysed. The results of the research have established uncertainties in the functioning of such components as the condensation column (CC) and low-temperature evaporators (LTE), which are connected to the operating circuit of two absorption refrigeration units (ARU) and TRU.

Algorithms have been developed for forming an information array of experimental data and numerical assessment of uncertainties, in particular heat transfer coefficients in the CC and LTE, as well as ammonia concentration at the outlet of the primary condensation unit and CC. The algorithms provide for the separation of transient modes in the operation of the TCSC, verification of stationarity, reproducibility of the process and the hypothesis of normality of empirical distribution, which determines the possibility of using a stochastic approximation method for numerical estimation of uncertainties.

Based on the results of processing the experimental data, a discrepancy between the actual and design heat transfer coefficients was established, which is due to an underestimation of the condensation thermal resistance. The heat exchange processes in the CC and LTE as part of the ARU were identified, and equations were obtained for determining the heat transfer coefficients, heat transfer, condensation thermal resistance, and ammonia concentration in the CG at the CC inlet and outlet.

Mathematical modelling was used to determine the conditions for the necessary temperature distribution in the TCSC to exclude the TRU from the circuit and reduce the cooling temperature of the CG in the LTE by 5°C compared to the initial version at maximum heat load from the CG at the inlet of the complex. The developed TCSC scheme is characterised by greater energy efficiency due to the use of only heat-utilising

refrigeration systems of the ARU and steam ejector units (SEU), which utilise the heat of material flows with both low temperature potential (up to 150°C) and ultra-low (up to 90°C).

Using mathematical modelling of LTE, a pattern of extreme dependence of cooling capacity and cooling temperature of the central heating system on the phlegm flow rate has been established. Achieving maximum cooling capacity, and therefore minimum cooling temperature of the central heating system at a certain temperature head, is determined by the critical regime of bubble boiling of the refrigerant. The dependencies of the cooling temperature of the central heating system on the control action of the phlegm flow rate have been determined, which characterise the shift of the extreme under conditions of changing values of the disturbance vector coordinates, and, consequently, the change in the energy efficiency indicators of ammonia production (annual natural gas consumption).

Algorithmic support has been developed to solve the problems of identification, obtaining a mathematical model of the LTE evaporator and numerical estimation of the optimal state vector (cooling temperature of the central heating system). The use of the algorithm implemented in the MATLAB package provides a solution to the optimisation problem in real time using a step-type non-gradient method with the application of one-dimensional extremum search methods. The technical structure of a computer-integrated system for optimal software control of the temperature regime of a low-temperature evaporator, adapted to the existing information system of an industrial synthesis unit, has been determined.

KEYWORDS

Ammonia production, secondary condensation, mathematical modelling of heat transfer processes, computer-integrated technology, optimal software control.

Synthetic ammonia is the most important product of the chemical industry. The continuous increase in the production of this product is due to the need to increase crop yields by applying nitrogen-containing mineral fertilisers to the soil. This need, in turn, is linked to the expected growth of the world population to almost 9.6 billion by 2050 [1]. Considering the latter and the availability of large amounts of arable land, ammonia and fertilisers will always be strategic commodities for Ukraine, determining the economic security of the state. At the same time, the main raw material in ammonia production technology is and will remain natural gas in the coming decades, which, compared to heavy oil and coal as raw materials, reduces energy costs by 1.3 and 1.7 times, respectively [2].

Modern ammonia synthesis units are complex energy-technological complexes with a large number of interconnected departments. Despite the diversity of equipment and technology, catalysts and equipment used to implement the processes, they are built in almost all countries according to the unified ideology of Kellogg Braun & Root (USA). The synthesis unit is based on the traditional Haber-Bosch closed circulation scheme with a two-stage system for condensing production ammonia from circulation gas [3].

The nitrogen industry in Ukraine is based on medium-pressure synthesis units with a capacity of 1,360 tons per day (AM-1360 series), which are significantly inferior in terms of energy consumption to

technologies from such world-renowned manufacturers as Haldor Topsoe (Denmark), Imperial Chemical Industries (UK), and Kellogg Braun & Root (USA), by almost 25% [4], and more than twice as much in terms of electricity consumption. At the same time, the efficiency of the units of leading manufacturers is largely achieved by the use of secondary condensation (TCSC) in the technological complex to drive turbo compressor cooling systems with medium pressure water vapor extraction (4 MPa), which is obtained by utilizing high-potential heat at the reforming stages and conducting ammonia synthesis at a lower pressure of up to 15 MPa [5]. The use of such technology directly in units operating in Ukraine is impossible due to the higher synthesis pressure (over 20 MPa). In such circumstances, there is not enough steam to drive the compressor systems. The insufficient amount of steam is obtained in an additional steam boiler, which significantly reduces the efficiency of domestic units. Therefore, in AM-1360 series synthesis units, a turbo compressor refrigeration unit (TRU) is used in addition to two low-temperature evaporators (LTE), along with two heat-using absorption refrigeration units (ARU), a turbo compressor refrigeration unit (TRU) with an electric drive is also used, the share of electricity of which is up to 40% of the total consumption of the entire production.

The simplest option for improving production efficiency would be to use a third ARU instead of a TRU. However, this is impossible due to the lack of units from both domestic and leading manufacturers that utilize waste heat streams with temperatures above 1000°C, which are necessary for the operation of the ARU by supplying heat to its generator-rectifier. In such circumstances, an alternative to ARU and TRU could be steam ejector refrigeration units (SEU), which, when using a refrigerant (ammonia) with a low boiling point, allow the utilization of heat from material flows with temperatures even below 900°C. However, today, in all synthesis units without exception, this heat is not utilized and is discharged into the environment through air cooling devices [6].

SEUs, compared to ARUs and TRUs, are characterized by lower thermodynamic efficiency. It can be increased by increasing the pressure and boiling point of the refrigerant in the evaporator [7]. However, recommendations on the possibility of using SEUs in chemical production, in particular ammonia, are practically absent in the literature. Therefore, this work focuses on research into the possibility of using SEUs for cooling the central gas in the general scheme of the AM-1360 series TCSC unit, the results of which can be applied to improve the technological design of cooling systems for synthesis units of various leading manufacturers in order to increase their energy efficiency by replacing complex and powerful steam-driven turbo compressor refrigeration systems. At the same time, the 4 MPa pressure water vapor from these units can be used to generate electricity, which will further increase their energy efficiency.

A characteristic feature of the TCSC is the presence of a condensation column. In this case, the direct flow of the heat transfer fluid at the inlet of the condensation column (CC) goes through the intertube space to two evaporators of the high-pressure system. The return flow of the heat transfer fluid from these high-pressure systems is directed to the separation part of the CC, and then to its tube space. This flow direction ensures the regeneration of "cold" and the separation of condensed ammonia from the refrigerant, to which a fresh nitrogen-hydrogen mixture (NHM) is supplied through the condensate layer. The operation of the TCSC due to the use of air cooling in the complex of primary condensation and refrigerant condensation in the ARU leads to constant seasonal and daily changes in the heat load on the evaporators, and therefore

is characterized by instability. All this causes fluctuations in the cooling temperature of the central heating system (secondary condensation) within a fairly wide range from –80°C to 50°C and causes not only parametric uncertainty in the operation of the facility, but also, due to the large tonnage of production, leads to significant economic losses. According to research, an increase in this temperature by even 10°C leads to a decrease in the energy efficiency of production due to an increase in annual natural gas consumption by 307.3 thousand nm^3 [8]. Therefore, minimizing the secondary condensation temperature by removing the TRU from the TCSC operation scheme through the creation of a high-quality control system under external disturbances is a pressing issue in the overall process of improving the energy efficiency of ammonia production.

The most effective way to solve such a complex task is to apply a systematic approach, one of the main components of which is systemic-structural and systemic-control [9]. The first is aimed at identifying the optimal structure of the technological system, and the second is aimed at studying its functioning and creating an adaptive system of optimal software control under the influence of external and internal disturbances. The scientific basis for this approach to final decision-making on this complex task is mathematical modeling and process identification [10]. Therefore, based on a systematic approach and using the example of TCSC, this paper presents some of the results of the authors' research, focusing on: the specifics of operating conditions, the formation of information arrays of experimental data and parametric identification of non-stationary static objects; mathematical modeling of multidimensional objects with uncertainties; synthesis of an energy-efficient structure of a technological complex using heat-using refrigeration units and an adaptive system of optimal software control based on the estimation of state coordinates.

1.1 FEATURES OF OPERATING CONDITIONS AND FORMATION OF AN ARRAY OF EXPERIMENTAL DATA FOR A SECONDARY CONDENSATION TECHNOLOGICAL COMPLEX

The operation of the TCSC technological equipment takes place under conditions of seasonal and daily changes in thermal load, which is caused by the use of air-cooling devices and a separator in the previous primary condensation unit. Under such circumstances, the temperature and pressure of primary condensation are subject to random changes, which, as is known, determine the concentration at the outlet of this unit. At the same time, the temperature of the central heating system and the concentration of ammonia in the central heating system at the inlet of the complex vary in the ranges of 35–45°C and 9–12% vol., respectively, and, consequently, at the inlet of the evaporators. An increase in this concentration not only increases the heat load, but also reduces the heat transfer coefficient due to the formation of additional condensation thermal resistance [11]. In addition, to determine the heat flows in the condensation column, it is necessary to know the concentration of ammonia in the CG at the outlet of its pipe space [12]. The value of this concentration is determined by the efficiency of the separation process, the calculation of which cannot be performed using analytical methods and depends on many uncontrollable factors. This also causes uncertainty in this concentration. A numerical assessment of these uncertainties for such linear technological objects is most often performed using the stochastic approximation method [13, 14], which has been sufficiently tested in industrial conditions.

The simplest way to eliminate these uncertainties would be to use an automatic analyser. However, the conditions of measurement, namely the presence of ammonia in the form of a vapour-liquid mixture and excessively high pressure in the central heating system, prevent the use of this method. In this regard, it is no coincidence that on existing synthesis units, the measurement of ammonia concentration in the central heating system is carried out using laboratory analyses, which are performed periodically, only once a day. Under such conditions and existing daily fluctuations in atmospheric air temperature, this method leads to complete uncertainty in the concentration of ammonia in the CG at certain periods. This complicates the real-time identification of heat exchange processes in the mathematical model of both the LTE and the CC. Thus, the task of identifying the processes of the mathematical model is complicated by the presence of interrelated uncertainties in the concentration of ammonia and the heat transfer coefficient, the solution of which is of particular importance in the process of obtaining mathematical models of LTE and CC. However, information on the numerical assessment of interrelated uncertainties is not sufficiently covered in the literature [15] and requires the development of a separate research algorithm for its application in the creation of an adequate mathematical model.

The significant metal intensity of the technological equipment and the complexity of the technological design of the TCSC contribute to the excessive inertia of heat exchange processes. This is especially true for the CC, whose total mass is almost 300 tonnes and is characterised by feedback on the CG flow. Therefore, under certain conditions, a situation may arise that makes it impossible to adapt the parameter to its actual value. In such circumstances, the identification of non-stationary static technological objects for the purpose of numerical estimation of the heat transfer coefficient requires the creation of an algorithmic basis for separating transient modes.

Thus, the established relationship between the uncertainties of the heat transfer coefficient, the concentration of ammonia in the heat carrier at the inlet and outlet of the column, and the numerical evaluation of uncertainties under existing conditions are of particular importance in the overall process of creating an automated system for the operational generation of a mathematical model of the evaporator and condensation column.

The formation of an array of experimental data on the elimination of transient modes of operation of the TCSC industrial synthesis unit of the AM-1360 series was carried out using the TDC-3000 microprocessor information and control complex from Honeywell and, in part, laboratory analyses of ammonia concentrations in the central gas. The method for determining the concentration is based on the absorption of ammonia by water, followed by titration of the ammonia water with sulphuric acid. The concentration of ammonia was determined by the amount of acid used to titrate the ammonia water. A generalised diagram of the TCSC with the main parameter control points according to the technological regulations is shown in **Fig. 1.1**.

Samples for laboratory analysis to determine the composition of the CG (ammonia, argon, methane, nitrogen, hydrogen) at the inlet and outlet of the CC were taken once per shift (8 hours). Therefore, the frequency of collection of all other data on the parameters of the TCSC operation was also once per shift. The analyses were performed using a NeoCHROM (Ukraine) industrial chromatograph, and the ammonia content in the CG was determined analytically using a standard method in the workshop laboratory.

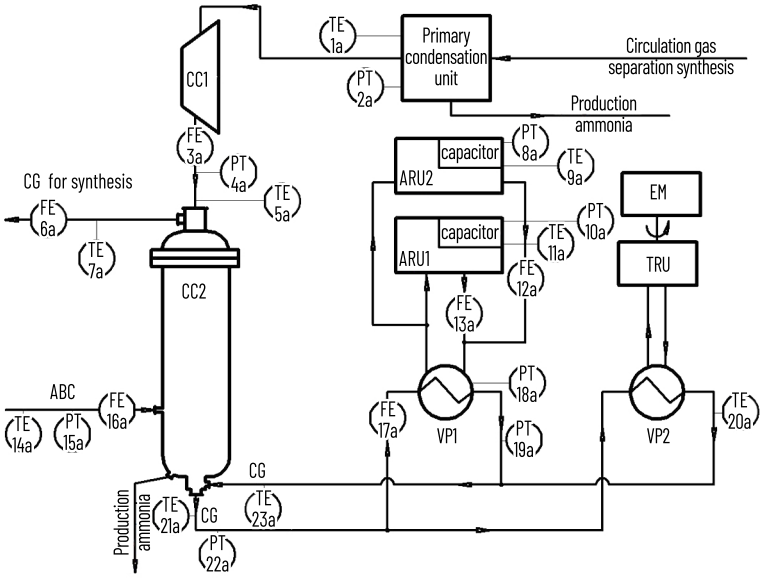

Fig. 1.1 Process diagram of the secondary condensation complex with the main parameter control points using the TDC-3000 information and control complex: CC1 — circulation compressor; CC2 — condensation column; VP1, VP2 — evaporator; ARU1, ARU2 — absorption refrigeration unit; TRU — turbo compressor refrigeration unit; EM — electric motor

In the process of developing the algorithm for forming the information array, equations of the mathematical description of the condensation column [16] were used, which, unlike the well-known ones, take into account both the condensation of ammonia in the intertube space and its evaporation in the tube space. The algorithm contains two convergence cycles. The first forms modes that ensure the convergence of heat flows due to heat exchange in the separation part due to heat exchange between the CG, the liquid ammonia layer and the NHM in order to determine the temperature of the CG at the inlet of the pipe space of the condensation column. The second cycle ensures the final formation of data on the input and output variables of the object under conditions of convergence of heat flows from the pipe and inter-pipe space of the heat exchange part of the condensation column. The algorithm includes the following main functional blocks [17]:

Block 1. Calling the task for solution after a specified period of time or at the operator's command.

Block 2. Opening the FORM file that serves this task.

Block 3. Subroutine for reading the necessary information from the DANI file, which stores information about the input and output variables and design characteristics of the object, obtained from the TDC-3000 information and control complex.

Blocks 4 and 5. Setting the initial temperature approximation $\Theta_{TP}^{C} = \Theta_{TP}^{B}$ with an approximation step of 0.001°C to determine the heat flows V_{ABC} (W) and V'_{ABC} (W) from NHM to the liquid ammonia layer and the heat source according to the equations:

$$\Phi_{ABC} = M_{ABC} C_{ABC} (\Theta_{ABC}^{C} - \Theta_{TP}^{C}); \tag{1.1}$$

$$\Phi'_{ABC} = \Phi_{MTP}^{C} + \Phi_{B}^{C}; \tag{1.2}$$

$$\Phi_{MTP}^{C} = M_{MTP}^{C} C_{MTP}^{C} (\Theta_{TP}^{C} - \Theta_{TP}^{B}) + M_{B}^{C} r^{C} + M_{G}^{Caver} C_{G}^{C} (\Theta_{TP}^{C} - \Theta_{TP}^{B}); \tag{1.3}$$

$$\Phi_{B}^{C} = G_{B}^{C} r^{C}; \tag{1.4}$$

$$G_{B}^{C} = V_{ABC} \frac{a_{NH_3}^{C} 0.771}{100 - a_{NH_3}^{C}}, \tag{1.5}$$

where Φ_{ABC}, Φ_{B}^{C}, Φ_{MTP}^{C} – amount of heat transferred to NHM, evaporation due to heat exchange in the liquid ammonia layer and heating of the central heating system; C_{ABC}, C_{MTP}^{C}, C_{G}^{C} – average heat capacities of NHM, the gas phase of the central heating system and liquid ammonia in the central heating system flow from the evaporator, kJ/(kg °C); M_{ABC}, M_{MTP}^{C}, M_{B}^{C}, M_{G}^{Caver}, G_{B}^{C} – mass flow rates of NHM, evaporated ammonia in the CG stream, liquid ammonia in the CG stream and evaporated ammonia due to heat exchange in the liquid ammonia layer, kg/s; V_{ABC} – volumetric flow rate of NHM, nm^3/s; Θ_{ABC}^{C}, Θ_{TP}^{C}, Θ_{TP}^{B} – temperatures of NHM at the column inlet, CG at the inlet of the column heat exchanger tube space, and CG at the evaporator outlet, °C; $a_{NH_3}^{C}$ – ammonia concentration in the CG stream at the column outlet, % vol.; r^{C} – ammonia vaporisation heat, kJ/kg.

Block 6. Evaluation of the convergence condition error $\delta = \left(\Phi_{ABC}^{1} - \Phi_{ABC}\right) < 3\%$ and transition to the second cycle if it is fulfilled.

Blocks 7 and 8. Determination of heat flows from the pipe side Φ_{TP}^{K} (W) and inter-pipe side Φ_{MTP}^{K} (W) of the heat exchanger space of the condensation column using the formulas:

$$\Phi_{TP}^{K} = M_{TP}^{G} C_{TP}^{C} (\Theta_{TP}^{K} - \Theta_{TP}^{C}) + M_{G}^{C} (i_{P}^{K} - i_{G}^{C}), \tag{1.6}$$

$$\Phi_{MTP}^{K} = M_{MTP}^{G} C_{MTP}^{C} (\Theta_{MTP}^{K} - \Theta_{MTP}^{B}) + M_{CK}^{K} r_{MTP} + (K_{G}^{K} - 0.5 M_{CK}^{K}) C_{G}^{C} (\Theta_{MTP}^{K} - \Theta_{MTP}^{B}), \tag{1.7}$$

where M_{TP}^{G}, M_{MTP}^{G} – gas phase flow rate of the central heating system, kg/s; M_{CK}^{K}, M_{G}^{K}, M_{G}^{C} – flow rates of condensed ammonia and liquid ammonia at the inlet between the intertube and tube space of the heat exchanger, kg/s; i_{P}^{K}, i_{G}^{C} – enthalpy of vapour and liquid ammonia at the inlet and outlet of the tube space of the heat exchanger, kJ/kg; C_{G}^{C}, C_{MTP}^{C}, C_{TP}^{G} – average heat capacities of liquid ammonia in the intertube space, gas phases of the intertube and tube space of the heat exchanger, kJ/(kg °C); r_{MTP} – heat of condensation of ammonia, kJ/kg; Θ_{TP}^{K}, Θ_{MTP}^{K}, Θ_{MTP}^{B} – temperatures of the heat transfer medium at the outlet of the pipe space, at the inlet and outlet of the intertube space of the heat exchanger, °C.

Block 9. Evaluation of the convergence condition error $\delta_2 = \left(\Phi^K_{MTP} - \Phi^K_{TP}\right) < 5\%$, in which case the transition to the calculation of heat transfer coefficients is carried out.

Block 10. Calculation of heat flow Φ^K heat transfer coefficients using the formulas adopted in the design K^K_P and the actual coefficient K^K_E for the condensation column:

$$K^K_P = \frac{1}{\frac{1}{a_{MTP}} + R^P_T + \frac{1}{a_{TP}}}; \tag{1.8}$$

$$K^K_E = \frac{\Phi^K}{F\Delta\Theta_{CP}}; \tag{1.9}$$

$$a_{MTP} = 1.3A\varepsilon_f (W_{MTP})^{0.56} (d_{OUT})^{-0.44}; \tag{1.10}$$

$$a_{TP} = A(W_{TP})^{0.8} (d_{IN})^{-0.2}; \tag{1.11}$$

$$\Phi^K = 0.5\left(\Phi^K_{TP} + \Phi^K_{MTP}\right), \tag{1.12}$$

where a_{TP} – heat transfer coefficients from the pipe and inter-pipe space, W/(m^2/°C); R^P_T = 0.000354 – design thermal resistance coefficient, m^2·K/W; $\Delta\Theta_{CP}$ – average temperature difference, °C; F – heat transfer surface, m^2; W_{TP}, W_{MTP} – weight velocity of the coolant in the pipe and inter-pipe space per unit of surface, kg/(m^2·s); ε_f – correction coefficient for the angle of attack; d_{IN}, d_{OUT} – internal and external diameter of heat exchange pipes, m; A – coefficient that takes into account the thermophysical properties of the heat transfer medium.

Block 11. Calculation of heat flow Φ_0, heat transfer coefficients according to the formulas adopted in the design K^B_P and the actual coefficient K^B_E for the evaporator:

$$K^B_E = \frac{\Phi_0}{F \cdot \Delta\Theta_{CP}}; \tag{1.13}$$

$$\Phi_0 = M_G C^{CP}_G \left(\Theta_{1C} - \Theta_{2C}\right) + M_{KC} C^{CP}_K \left(\Theta_{1C} - \Theta_{2C}\right) + M_K r^{CP} + M^{OUT}_P C^{aver}_P \left(\Theta_{1C} - \Theta_{2C}\right); \tag{1.14}$$

$$M_K = 0.771 \cdot V_C \left(a^{PIN}_{NH_3} - a^{POUT}_{NH_3}\right); \tag{1.15}$$

$$K^B_P = \frac{1}{\frac{1}{a_{MTP}} + R^P_T + \frac{1}{a_{TP}}}; \tag{1.16}$$

$$a_{TP} = A \cdot W^{0.8}_{TP} \cdot d^{-0.2}_{IN}; \tag{1.17}$$

$$a_{MTP} = 2.2 \cdot q^{0.7}_F \cdot P^{0.21}_{MTP}; \tag{1.18}$$

$$A = 16.28 \cdot \left(\frac{\lambda_C}{\mu_C^{0.8}} \right) \cdot \left(\frac{Pr}{0.73} \right)^{0.4}, \quad (1.19)$$

where W_{TP} is the weight velocity of the coolant per unit surface area in the pipe space, kg/(m^2·s); d_{IN} is the internal diameter of the pipes, m; q_F is the specific heat flux, W/m^2; λ_C is the thermal conductivity of the coolant, W/(m·K); μ_C is the dynamic viscosity of the coolant, Pa·s; Pr is the Prandtl number; $R_T^P = 0.000356$ is thermal resistance coefficient, m^2·K/W; Φ_0 is heat flux (cooling capacity), W; F is evaporator heat transfer surface, m^2; Θ_{CP} is mean logarithmic temperature difference, °C; M_G, M_{KS}, M_K, M_P are mass flow rate of the gas phase of the refrigeration circuit, average ammonia condensate, condensed ammonia and ammonia vapour phase in the refrigeration circuit, kg/s; C_G^{CP}, C_K^{CP}, C_P^{CP} are average specific heat capacities of the gas phase of the central heating system, ammonia condensate and ammonia vapour, kJ/(kg·K); r_{CP} is average heat of condensation of ammonia, kJ/kg; Θ_{1C}, Θ_{2C} are temperature of the refrigerant at the evaporator inlet and outlet, °C; V_C is volumetric flow rate of the refrigerant, nm^3/s; $a_{NH_3}^{PIN}$, $a_{NH_3}^{POUT}$ are concentration of ammonia vapour in the refrigerant at the inlet and outlet, % vol.

Block 12. The discrepancy between the design and actual heat transfer efficiency indicators was assessed by the total thermal resistance R_E^T for the evaporator and condensation column using the formula

$$R_E^T = \frac{1}{K_E} - \left[\frac{1}{a_{MTP}} + \frac{1}{a_{TP}} \right]. \quad (1.20)$$

Block 13. Formation of an array of current STAB data of stable values of object quantities with respect to Φ_{ABC}, Φ^K, Φ_0, R_E^T, M_{KC}, M_{CK}, K_P, K_E and technological parameters, and printing of results.

Block 14. Closing the FORM file and exiting the task.

The developed algorithm structure allows forming a stable information array of current data and separating transient modes. This makes it possible to calculate the actual heat transfer coefficient and, consequently, the condensation thermal resistance.

The possibility of applying a probabilistic-statistical (stochastic) approach for numerical estimation of uncertainties requires, as is known, verification of a number of conditions [6, 18]. In order to implement such verification, algorithmic support has been developed for processing experimental data obtained at the previous stage of forming the information array. The algorithm ensures verification of the stationarity and reproducibility of the process, the hypothesis of the normality of the empirical distribution, and the approximation of ammonia concentrations in the central gas according to the functional dependence established in accordance with existing theoretical provisions. The algorithm includes the following functional blocks [19]:

Block 1. Calling the task to be solved after a specified period of time or at the operator's command.

Block 2. Open the STOCH program file that serves this task.

Block 3. Subroutine for reading the necessary information from the STAB file, which stores information about the input and output variables of the TCSC obtained in the process of forming the information array.

Block 4. For each independent variable, the number of series of experiments $i = 1 \div k$ is determined, into which the experimental data is divided, as well as the number of experimental data $j = 1 \div m$ in each series ($i = 4$, $j = 3$).

Blocks 5 and 6. Calculation of the Cochran criterion G_p to verify the reproducibility of the process, establishment of the tabulated value G_T with the number of degrees of freedom k, m and a significance level of 5% with verification of the reproducibility condition using the formulas:

$$G_p = \frac{max\left\{\sigma_i^2(a)\right\}}{S_a^2}; \tag{1.21}$$

$$S_a^2 = \sum_{i=1}^{k}\sigma_i^2(a); \tag{1.22}$$

$$\sigma_i^2(a) = \frac{1}{m-1}\sum_{j=1}^{m}\left(a^{ij} - \overline{a^i}\right)^2; \tag{1.23}$$

$$\overline{a^i} = \frac{1}{m}\sum_{j=1}^{m}a^{ij}; \tag{1.24}$$

$$G_P < G_T. \tag{1.25}$$

Block 7 and 8. Calculation of Fisher's criterion F_p to verify the stationarity of the process, establish a tabulated value for the number of degrees of freedom and a significance level of 5% with verification of the stationarity condition using the equations:

$$F_p = \sigma_\Sigma^2 / \sigma_0^2; \tag{1.26}$$

$$\sigma_0 = S_a^2 / k; \tag{1.27}$$

$$\sigma_\Sigma^2 = \frac{m}{k-1}\sum_{i=1}^{k}\left(\overline{a^i} - \overline{a^{ij}}\right); \tag{1.28}$$

$$\overline{a^{ij}} = \frac{1}{k}\sum_{i=1}^{k}\overline{a^i}; \tag{1.29}$$

$$F_P < F_T. \tag{1.30}$$

Block 9. Determination of sample asymmetry A and excess E, as well as theoretical dispersion of asymmetry $\sigma(A)$ and excess $\sigma(E)$ using the following formulas:

$$A = \frac{1}{N\cdot\sigma_a^3}\sum_{u=1}^{N}\left(a_u - \overline{a_u}\right)^3; \tag{1.31}$$

$$E = \frac{1}{N\cdot\sigma_a^4}\sum_{u=1}^{N}\left(a_u - \overline{a_u}\right)^4 - 3; \tag{1.32}$$

$$\sigma(A) = \frac{6(N-1)}{(N+1)(N+3)}; \tag{1.33}$$

$$\sigma(E) = \frac{24N(N-2)(N-3)}{(N+1)^2(N+3)(N+5)}, \tag{1.34}$$

where σ_a is the standard deviation of the output parameter relative to the mean.

Block 10. Verification of the hypothesis of normality of the empirical distribution, which is accepted if the following conditions are met:

$$|A| \le 3\sqrt{\sigma(A)}; \tag{1.35}$$

$$|E| \le 5\sqrt{\sigma(E)}. \tag{1.36}$$

Block 11. If the above conditions are met, close the STOCH file and exit the task.

Based on the results of processing the experimental data using the above algorithms, a sample of 100 TCSC operating modes was formed, some of which are presented in **Tables 1.1** and **1.2**.

As an example, **Table 1.3** presents selected results of the quality check of the obtained data set. Analysis of these results shows that the process in the selected time interval is sufficiently reproducible and stationary, and the empirical distribution practically corresponds to the normal law.

The developed algorithm structure allows switching to Statistica or MATLAB (Optimisation Toolbox) packages to perform correlation and regression analysis and determine functional dependencies for numerical estimates of ammonia concentrations in the central gas at the outlet of the primary condensation unit (inlet to the condenser) $a^{IN}_{NH_3}$ and at the outlet of the pipe space of the condensation column $a^{TP}_{NH_3}$, which, according to existing theoretical provisions, should be searched for using the following equations:

$$a^{in}_{NH_3} = f\left(P_{TP}, \Theta_{TP}\right); \tag{1.37}$$

$$a^{TP}_{NH_3} = f\left(V_{ABC}, V^{C}_{MTP}, \Theta^{B}_{TP}, a^{IN}_{NH_3}, P\right), \tag{1.38}$$

where P_{TP}, Θ_{TP} – pressure and temperature of primary condensation, respectively; V_{ABC} – NHM flow rate; V^{C}_{MTP} – CG flow rate in the intertube space of the column; Θ^{B}_{TP} – CG temperature at the evaporator outlet; P – CG pressure.

Table 1.1 Experimental data on the operating modes of the condensation column

Parameter names			Mode numbers						
			1	2	3	4	5	6	7
Circulation gas at the column inlet	V^{C}_{MTP} flow rate $\cdot 10^3$, nm^3/hour		639.23	621.25	627.08	625.53	621.59	613.08	613.08
	Pressure P_C, MPa		24	22.4	23	23.0	22.8	22.2	22.2
	Temperature Θ^{K}_{MTP}, °C		37	42	35	40	39	34	40
	Concentration, % vol.	hydrogen $a^{MTP}_{H_2}$	55.7	55.9	55.7	56.5	54.4	55.2	55.6
		methane $a^{MTP}_{H_4}$	8.4	8.0	8	8.2	8.2	8.2	7.8
		nitrogen $a^{MTP}_{H_2}$	18.9	19.6	20.0	19.0	19.5	18.7	18.9
		argon a^{MTP}_{Ar}	6.9	6.8	7	7.9	7.6	7.6	7
		ammonia $a^{MTP}_{NH_3}$	10.1	8.6	9.3	8.4	10.3	10.3	10.4
Nitrogen-hydrogen mixture at the separator inlet	Flow rate $V_{NHM} \cdot 10^3$, nm^3/hour		174	175	175	176	174	173	169
	Pressure P_{NHM}, MPa		24.2	23.2	24	23.5	23.2	23.2	23.2
	Temperature Θ^{C}_{ABC}, °C		35	36	35	41	43	36	40
Temperature Θ^{B}_{MTP}, °C			16	19	13	17	16	12	17
Central heating temperature at the evaporator outlet, Θ^{B}_{TP}, °C			–0.5	–	–	–5	–6	–7	–4
Circulation gas at the column outlet	V^{C}_{TP} flow rate $\cdot 10^3$, nm^3/hour		774.2	771.35	770.7	776.1	758.08	747.58	745.12
	Temperature Θ^{K}_{TP}, °C		25	24	22	24	24	21	24
	Concentration, % vol	hydrogen $a^{TP}_{H_2}$	62.2	62.3	61.7	62.4	62.3	61.9	62.8
		methane $a^{TP}_{CH_4}$	7.2	6.8	6.9	6.9	7.1	7	6.5
		nitrogen $a^{TP}_{N_2}$	21.3	21.3	21.9	20.6	20.5	21.2	20.8
		argon a^{TP}_{Ar}	6.0	5.9	6.0	6.6	6.6	6.6	6.3
		ammonia $a^{TP}_{NH_3}$	3.3	3.7	3.5	3.5	3.5	3.3	3.6

Note: NHM composition (% vol.) – $a^{ABC}_{H_2} = 76.3$; $a^{ABC}_{CH_4} = 0.4$; $a^{ABC}_{N_2} = 23.2$; $a^{ABC}_{Ar} = 0.1$
Source: [16]

Table 1.2 Experimental data on the operating modes of the primary condensation unit and the ARU evaporator

Parameter names			Mode numbers						
			1	2	3	4	5	6	7
CG at the outlet of the primary condensation unit	Flow rate $V_{0C} \cdot 10^{-3}$, nm³/hour		639.2	638.4	643.4	631	623.4	640.0	634.8
	Pressure P_{PC}, MPa		22.1	22	22	22.0	22.7	22.4	24
	Temperature ΘP_C, °C		28	36	29	30	25	29	22
	Concentration,% vol.	$a^{IN}_{H_2}$	55.7	56	55.6	56.8	57.2	56.2	56.2
		$a^{IN}_{N_2}$	18.9	18.9	19.2	17.6	18.8	19.5	20
		$a^{IN}_{CH_4}$	8.4	8.3	8.7	8.8	8	7.7	8.4
		a^{IN}_{Ar}	6.9	6.9	6.7	6.8	6.9	6.8	7.3
		$a^{IN}_{NH_3}$	10.1	9.9	9.8	10	9.1	9.8	8.1
Central heating temperature	at the evaporator inlet Θ_{1C}, °C		16	23	15	18	13	18	18
	at the evaporator outlet Θ_{2C}, °C		–5	–1	–8	–6	–3	4	–6
Central heating consumption at the evaporator inlet $V_C \cdot 10^{-3}$, nm³/hour			319.6	316.2	321	315.5	311.7	320.0	317.4
Central heating pressure P_C, MPa			23.5	23	23	22.7	23.5	23.8	24.8
Intertube space of the evaporator when connected to a two-ARU circuit	Refrigerant boiling pressure P_{MTR}, MPa		0.19	0.25	0.17	0.2	0.2	0.25	0.20
	Refrigerant boiling point Θ_{MTR}, °C		–13	–8	–15	–13	–8	–2	–12
	Refrigerant concentration at inlet ξ^{IN}_X, kg/kg		0.989	0.991	0.993	0.995	0.997	0.996	0.995
	Phlegm consumption M_F, t/year		0.902	1.158	0.541	0.465	0.102	0.142	0.937
	Refrigerant consumption at the inlet M^{IN}_X, t/year		15.995	19.174	16.885	17.507	10.878	10.410	17.313
	Liquid refrigerant inlet temperature Θ^{IN}_X, °C		26	28	29	27	20	25	27

*Note:*there was one ARU in operation*
Source: [19]

Table 1.3 Generalised indicators of the quality of the information obtained

Indicator name		Designation	Numerical value
Average concentration		$\overline{a_{ij}}$	9.85
Maximum sample variance for a single series		$\sigma_i^2(a)$	0.45
Total sum of variances		S_a^2	1.002
Cochran's criterion	calculated	G_p	0.4491
	tabulated	G_m	0.6841
Reproducibility dispersion		σ_0^2	0.25
Residual dispersion		σ_Σ^2	0.2041
Fisher's criterion	calculated	F_p	0.8164
	tabulated	F_B	8.84
Selective	asymmetry	$\lvert A\rvert$	$1.037 \cdot 10^{-3}$
Excess		$\lvert E\rvert$	2.999
Condition for theoretical dispersions	asymmetry	$3\sqrt{\sigma(A)}$	0.644
	of excess	$5\sqrt{\sigma(E)}$	2.064

Source: [19]

1.2 IDENTIFICATION OF HEAT EXCHANGE AND CONDENSATION–SEPARATION PROCESSES IN THE SECONDARY CONDENSATION PROCESS COMPLEX

In order to solve the problem of identifying heat exchange processes in the CC, calculations were made of the total actual thermal resistance R_T^E, the actual heat transfer coefficient K_E^K and the design coefficient K_P^K using equations (1.6)–(1.11), (1.20) given in Section 1.1 of the algorithm for forming the information array. The calculation results are summarised in **Tables 1.4** and **1.5**, where the mode numbers correspond to the numbers in **Table 1.1**.

As can be seen from **Tables 1.4** and **1.5**, the heat transfer coefficient in real conditions K_E^K is almost two times less than the coefficient K_P^K calculated using the equations adopted in the design. According to existing theoretical provisions [20], this discrepancy is due to the presence of additional condensation thermal resistance.

Table 1.4 Results of calculations of the actual heat transfer coefficient of the condensation column based on experimental data

Parameter names			Mode numbers						
			1	2	3	4	5	6	7
Heat flows, MW	Separation section	Φ^C_{ABC}	2.128	2.302	2.233	2.733	2.861	2.512	2.535
		Φ^C_{MTP}	0.523	0.488	0.523	1.000	1.139	0.895	0.814
		Φ^C_B	1.605	1.826	1.721	1.732	1.721	1.616	1.709
	Heat exchanger	Φ^K_{TP}	9.687	10.595	9.687	10.932	10.978	10.187	10.443
		Φ^K_{MTP}	9.874	11.129	10.048	10.804	10.850	9.955	10.932
Θ^C_{TP}, at the outlet of the separation section, °C			0.89	–0.68	–0.61	–2.23	–2.84	–4.5	–1.75
Heat balance discrepancy, %			1.9	4.9	3.8	1.7	1.1	2.2	4.7
Heat transfer coefficient K^K_E, W/m²·K			340.3	271.9	349.9	292.1	304.2	322.3	290.1
Condensed ammonia consumption M_{SK}, t/year			14.4	18.1	14	16.9	16.6	14.43	17

Source: [16]

Table 1.5 Results of calculations of the efficiency indicators of the heat exchange process of the condensation column according to the design and actual thermal resistance

Name of parameters	Mode numbers						
	1	2	3	4	5	6	7
Heat transfer coefficient α_{TP}, W/m²·K	1790.12	1780.65	1801.8	1797.95	1764.68	1761.93	1727.63
Heat transfer coefficient α_{MTP}, W/m²·K	1454.49	1418.31	1447.51	1443.06	1460.13	1431.65	1423.98
Heat transfer coefficient K^K_P, W/m²·K	645	636.91	645.39	644.32	642.89	636.91	635.52
Total thermal resistance R^E_T, m²·K/W	0.00169	0.00241	0.00161	0.00217	0.00203	0.00183	0.00216

Source: [16]

The calculated values in **Table 1.4** and **1.5** show that there is a non-random relationship between the total thermal resistance coefficient R^E_T and the consumption of condensed ammonia M_{CK}. Based on the

results of processing these indicators using the least squares method, an equation was obtained for the numerical estimation of the uncertainty of this coefficient [21]

$$R_T^E = 2.102 \cdot 10^{-5} \cdot M_{CK}^2 - 0.0004674 \cdot M_{CK} + 0.0040679. \quad (1.39)$$

The error in calculations using equation (1.39) does not exceed 6%.

The identification of the heat exchange process in the evaporator was performed using an experimental data set, some of which are presented in **Table 1.2**. The results of calculations of the heat transfer coefficient K_E and the total thermal resistance R_T^E according to equations (1.13)–(1.19) are summarised in **Table 1.6**, where the mode numbers correspond to the numbers in **Table 1.2**.

Table 1.6 Efficiency indicators of the heat exchange process of the ARU evaporator according to experimental data

Name of indicators	Mode numbers						
	1	2	3	4	5	6	7
Cooling capacity Φ_0, MW	4.59	5.53	5.01	5.24	3.38	3.23	5.22
Average consumption of ammonia condensate M_{KS}, t/year	19.1	16.78	18	18.04	16.1	17.7	13.2
Heat transfer coefficient α_{MTR}, W/(m^2·K)	1310.3	1581.6	1360.5	1453.2	1069.3	1085.3	1448.8
Heat transfer coefficient α_{TP}, W/(m^2·K)	3917.3	3889.6	3932.1	3779.7	3783.9	3915.8	3929.7
Total thermal resistance $R_T^{\text{Å}} \cdot 10^4$, (m^2·K)/W	8.2631	6.2330	6.4841	6.4540	5.1315	6.9836	5.3671
Heat transfer coefficient K_E, W/(m^2·K)	541.6	660.4	610.1	625.7	584.2	533.2	673.8

Source: [19]

As can be seen from **Table 1.6**, the heat transfer coefficient in real conditions K_E is on average almost 1.8 times less than the coefficient K_P = 1130.4 W/(m^2·K), calculated using equations (1.16)–(1.19) accepted in the design, and the total thermal resistance R_T^P at the level of 0.000356 (m^2·K)/W. As in the previous case, this discrepancy is due to the presence of additional condensation thermal resistance. A numerical estimate of this resistance based on the approximation results can be represented by the following equation

$$R_T^E = \left(0.0956 M_{KC}^2 - 2.5111 M_{KC} + 21.081\right) 10^{-4}. \quad (1.40)$$

The error in calculations using equation (1.40) does not exceed 14%.

Based on the results of processing experimental data on ammonia concentration $a_{NH_3}^{IN}$ at the inlet (**Table 2.4**) and outlet $a_{NH_3}^{OUT}$ of the heat exchanger using the MATLAB package, the following equations were obtained for their numerical estimation, which have the following form [19, 21]:

$$a_{NH_3}^{IN} = 22.068 - 0.6272P_{TP} + 0.05245\Theta_{TP}; \quad (1.41)$$

$$a_{NH_3}^{TP} = -7.78 + 0.02441 \cdot V_{ABC} + 0.01176 \cdot V_{MTP}^{C} + \\ +0.0327 \cdot \left(\Theta_{TP}^{B} + 273\right) + 0.085 \cdot a_{NH_3}^{MTP} - 0.0635 \cdot P. \quad (1.42)$$

The error in calculations using equations (1.41) and (1.42) does not exceed 6%.

1.3 SYNTHESIS OF THE HARDWARE AND TECHNOLOGICAL DESIGN OF THE SECONDARY CONDENSATION COMPLEX AND DETERMINATION OF THE GENERAL STRUCTURE OF ITS CONTROL SYSTEM

Equations (1.1)–(1.7), (1.10), (1.11), (1.20), (1.39) and (1.42), obtained as a result of the identification of heat exchange processes, constitute a mathematical model of the condensation column.

Table 1.7 presents some of the results of calculating the target indicators for the CC operating modes obtained in the process of mathematical modelling. The mode numbers in **Table 1.7** correspond to the numbers in **Table 1.1.**

Table 1.7 Main target indicators of the condensation column operating modes based on the results of mathematical modelling

Heat transfer efficiency indicators	Mode numbers						
	1	2	3	4	5	6	7
Heat flow of the separation part Φ^{C}, MW	2.162	2.298	2.248	2.729	2.78	2.534	2.536
Heat flow of the heat exchanger Φ^{K}, MW	10.22	10.772	9.927	10.855	10.929	10.604	10.690
Heat transfer coefficient of the heat exchanger K, W/m^2·K	332.51	275.67	339.29	289.8	296.31	324.48	289.61
Circulation gas consumption at the pipe space outlet $V_{TP}^{C} \cdot 10^3$, nm^3/hour	777.67	770.59	771.89	775.93	758.78	749.59	745.42
Circulation gas temperature at the outlet of the pipe space Θ_{TP}^{K}, °C	22.8	25.5	21.5	23.7	22.9	20	24.5
Circulation gas temperature at the inlet to the pipe space Θ_{TP}^{C}, °C	0.896	–0.575	–0.774	–2.194	–2.948	–4.8	–1.8
Temperature of the circulating gas at the evaporator inlet Θ_{MTP}^{B}, °C	15.17	19	13	16.9	15.8	10.4	17.6
Ammonia concentration in the circulating gas at the outlet of the pipe space, $a_{NH_3}^{TP}$, % vol.	3.7	3.6	3.6	3.4	3.59	3.56	3.6

Source: [16]

A comparison of experimental data (**Table 1.4**) and data obtained during modelling (**Table 1.7**) shows that the calculation error does not exceed the approximation error according to equations (1.39) and (1.42), i.e. 6%. Such convergence allows us to conclude that it is possible to use the mathematical model of CC for the synthesis of the technical structure of increased energy efficiency of TCSC.

Fig. 1.2 shows some of the results of mathematical modelling of the CC. They allow us to quantitatively assess the increase in thermal load on the LTE evaporators under real operating conditions compared to those assumed in the design. The dependencies shown in **Fig. 1.2** were obtained at a maximum CG inlet temperature of 45°C, which is observed in real conditions.

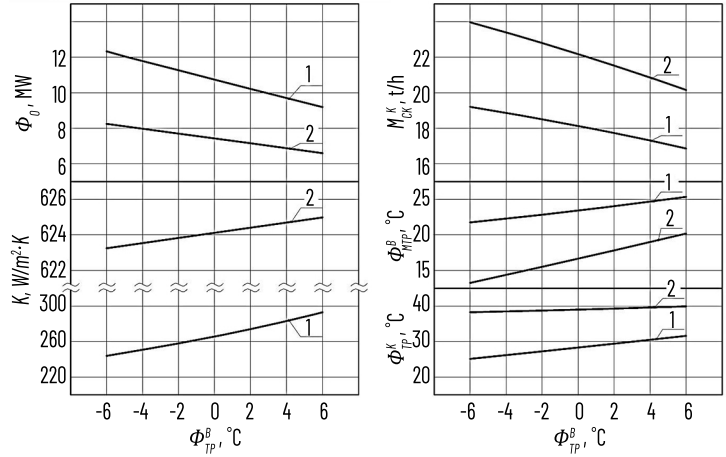

Fig. 1.2 Dependence of individual indicators of heat exchange efficiency in the condensation column and cooling capacity of refrigeration systems on the cooling temperature of the circulating gas in the evaporators for the initial data of mode No. 5 in **Table 1.1**

Source: [16]

According to **Fig. 1.2**, maintaining the specified temperature at 5°C requires an increase in the cooling capacity of refrigeration systems by 4 MW relative to the design value of 8.12 MW. This increase is due to a decrease in the actual heat transfer coefficient K_E to 247.7 W/m^2·K compared to the coefficient K_P = 623.4 W/m^2·K, which is due to the presence of additional condensation thermal resistance due to ammonia condensation M_{SK}. As a result, there is an increase in the temperature Θ^B_{MTP} at the inlet of low-temperature evaporators from 13.8°C to 22°C and a decrease in the temperature Θ^K_{TP}, at the outlet of the CC tube space from 38.4°C to 25.7°C.

The dependencies shown in **Fig. 1.3** and **1.4** allow us to determine the conditions (shown in dotted lines) for not only excluding the TRU from the synthesis unit operation scheme, but also reducing the cooling temperature of the CG in the evaporators (LTE1, LTE2) to a minimum level of 5°C using only two ARUs. However,

this requires a reduction in the heat load on the LTE evaporators in terms of temperature, which can be achieved by installing an additional heat exchanger (AH) for deeper cold recovery.

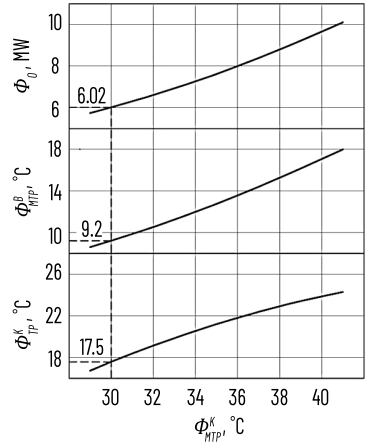

Fig. 1.3 Effect of circulation gas temperature at the inlet of the condensation column
Source: [16]

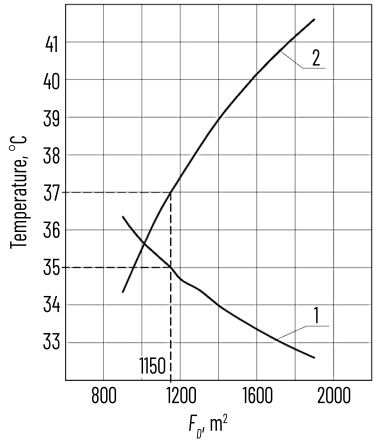

Fig. 1.4 Influence of the heat exchange surface of the additional heat exchanger *FD* on the distribution of temperatures at the outlets of the circulating gas at its maximum thermal load at the inlet temperature Θ^{IN}_{MTP} = 45°C
Source: [16]

Analysis of the dependencies shown in **Fig. 1.3** and **1.4** indicates that at a circulating gas temperature of Θ^{K}_{MTP} = 30°C at the inlet to the cooling unit, the cooling temperature can be stabilised at the minimum (regulatory) level of 5°C with only two automatic control units. At the same time, their cooling capacity must be even lower than the existing 6.28 MW, namely 6.02 MW. It is impossible to fulfil this condition even by installing a AH according to **Fig. 1.4**. Therefore, it is advisable to install a AH in front of the high-temperature evaporator (HTE) heat exchanger with a significantly smaller, i.e. optimal, heat exchange surface F_D = 1150 m^2. The boiling temperature of ammonia in the intertube space is not higher than 24°C, and the pressure of 0.9915 MPa ensures a decrease in the temperature of the direct flow of the cooling agent from 35°C to 30°C. The boiling temperature regime in the HTE can be ensured by connecting it to the cycle of the steam ejector refrigeration unit (SERU), as shown in **Fig. 1.5** [16, 21].

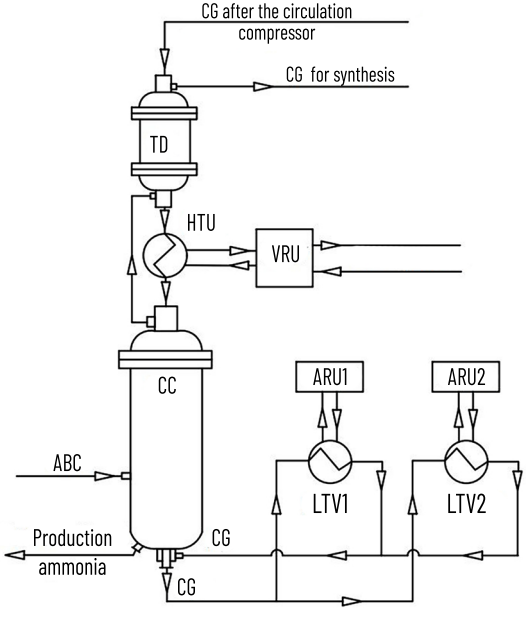

Fig. 1.5 Equipment and technological design of a secondary condensation complex with increased energy efficiency: CC — condensation column; CG — circulation gas; ABC — nitrogen-hydrogen mixture; ARU — absorption refrigeration unit; SEU — steam ejector refrigeration unit; HTE and LTE — high-temperature and low-temperature evaporators, respectively; AH — additional heat exchanger
Source: [21]

The injection coefficient of the SEU jet compressor was determined using a well-proven algorithm [22]. Due to the use of air-cooling devices in the SEU, the injection coefficient was set according to the achievable

compression pressure, the value of which was limited to 1.6 MPa. This allows even in the summer period to ensure a high temperature (40°C) of ammonia vapour condensation after the jet compressor.

According to the calculation results, the injection coefficient is at least 0.4. With this coefficient, 20 t/h of working steam from the SEU steam generator with a pressure of 3 MPa is sufficient to inject 8 t/h of ammonia steam from the HTE evaporator. This will provide a cooling capacity of 2.48 MW. The total amount of refrigerant steam and working steam for air condensers will be 28 t/h, the condensation of which can be provided by three condensers with an electricity consumption of 600 kWh. To obtain 20 t/h of working steam, 515 t/h of monoethanolamine (MEA) solution from the first stream of the MEA purification section through a steam generator is sufficient, i.e. 20·974.4/3.78·(85–75) = 515 t/h. The numerical values in this calculation are as follows: the specific heat of vaporisation of ammonia at a temperature of 65°C and a pressure of 3 MPa is 974.4 kJ/kg; the specific heat capacity of the MEA solution is 3.78 kJ/kg·K; the inlet and outlet temperatures of the MEA solution are 85°C and 75°C, respectively. Due to such heat utilisation, the load on the air coolers of this solution and heat emissions into the atmosphere are reduced.

This technological design allows reducing the total cooling capacity at the secondary condensation stage from 11.16 MW to 8.5 MW. This is due to deeper recovery and utilization of low-potential heat in the SEU with a MEA solution flow temperature of up to 90°C. At the same time, due to the exclusion of the TRU from the unit's operating scheme, electricity consumption will be reduced by 3.4 thousand kWh. Despite this reduction in cooling capacity, it is possible to reduce and stabilise the cooling temperature of the central heating system in the evaporators from 0°C to –5°C at its maximum temperature at the inlet to the condensation column. This maximum load is typical for the operation of the synthesis unit for about 4 months in the spring-summer period. A 5°C decrease in temperature during this period will also reduce natural gas consumption by 190 m^3/hour in an additional steam boiler for producing water vapour at a pressure of 10 MPa. This will result in annual natural gas savings of approximately 550 thousand nm^3. The advantage of the proposed structure is that it ensures the cooling temperature regime of the central heating system only with the help of heat-using refrigeration systems that utilise both low-temperature heat in the ARU and ultra-low-temperature heat in the SEU.

The central place in this TCSC structure is occupied by LTE evaporators, the efficiency of which ultimately determines the secondary condensation temperature. The evaporators are immersed shell-and-tube heat exchangers with U-shaped tubes. The CG is cooled in the tube space by ammonia boiling in the intertube space. The peculiarity of the evaporation process of liquid ammonia (refrigerant) is that it enters the evaporator with water impurities. To remove water, a process of draining phlegm from the evaporator is provided [23]. Insufficient phlegm drainage causes water to accumulate in the evaporator. This leads to a decrease in ammonia concentration, an increase in pressure and cooling temperature, and, consequently, a decrease in cooling capacity. Excessive drainage causes a loss of refrigerant, which reduces cooling capacity and cooling temperature. Thus, the phlegm flow rate $M_{\Phi}(t)$ is one of the main controlling influences of the control vector $Y(t)$, which determines the optimal state vector x^{OPT}. However, there is practically no information in periodicals on determining the quantitative dependence of the influence of the flow rate $M_{\Phi}(t)$ on the efficiency of the heat exchange process and, consequently, on the cooling temperature regime of the central heating system. This absence is due to the widespread use of ARU with low cooling capacity.

In such installations, periodic phlegm drainage is mainly carried out, and the impact of this process on the efficiency of production is not so significant [24]. For refrigeration units with high cooling capacity, over 3 MW, used in ammonia production, this impact can be quite significant. The task of determining the quantitative dependence of the control vector $M_{\phi}(t)$ on the optimal state vector x^{OPT} and creating an algorithm for optimisation can be most effectively solved using a mathematical model of the evaporator.

The purpose and place of the mathematical model is clearly illustrated by the generalised structure of the adaptive system for optimising the operating mode of the control object, shown in **Fig. 1.6** [25].

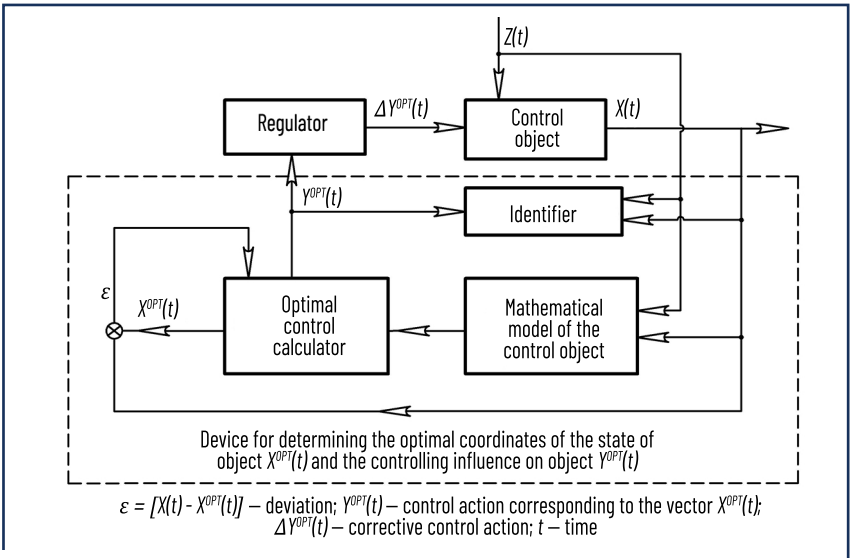

Fig. 1.6 Generalised structure of an adaptive system for optimising the operating mode of a control object
Source: [19]

With regard to the evaporator, the task of synthesising an algorithm for minimising the cooling temperature of the central heating system under certain constraints can be represented in general terms as follows:

$$\varphi\left(x,Y,z\right)\rightarrow min\left(extr\right)\Rightarrow x^{OPT}, \tag{1.43}$$

$$x=F\left(Y,z\right), \tag{1.44}$$

where φ is the objective function; x, z are the coordinate vectors corresponding to the state of the object and disturbances of a certain dimension; Y is the vector of control actions; F is the operator of the mathematical model of the evaporator.

The operation of the LTE evaporator is influenced by a large number of disturbance factors, both external from the primary condensation unit and internal from the ARU. All this will cause a shift in the optimal state coordinates (cooling temperature of the central heating system) and control action (phlegm flow rate). Determining these coordinates and identifying the patterns of the disturbance vector's influence on the shift of the optimal state coordinates can be achieved through mathematical modelling, which requires the construction of a mathematical model of the LTE and the development of algorithmic research tools.

1.4 INVESTIGATION OF THE PATTERNS OF INFLUENCE OF PHLEGM DRAINAGE INTENSITY ON THE EFFICIENCY OF THE CIRCULATING GAS COOLING PROCESS IN LOW-TEMPERATURE EVAPORATORS

In the process of developing a mathematical model of an evaporator, uncertainties in its description are due to a number of assumptions. Among them, the following can be highlighted: saturation of ammonia vapour throughout the entire intertube space, negligible heat of hydraulic losses, uniform distribution of ammonia concentration in the volume of boiling liquid, no formation of non-boiling liquid in the evaporator intertube space, and a mean logarithmic distribution of the temperature of the working fluid. Given these uncertainties, the mathematical description of the evaporator is based on well-known equations of heat transfer, material and energy balance. The main equations are as follows [19]:

$$\Phi_0 = M_\Phi i_\Phi + M_Y^{OUT} i_Y^{OUT} - M_X^{IN} i_X^{IN}; \tag{1.45}$$

$$M_X^{IN} \xi_X^{IN} = M_\Phi \xi_\Phi + M_Y^{OUT} \xi_Y^{OUT}; \tag{1.46}$$

$$M_X^{IN} = M_\Phi + M_Y^{OUT}; \tag{1.47}$$

$$\Phi_{MTP} = \alpha_{MTP} F_{MTP} \left(\Theta_{MTP}^{CT} - \Theta_{MTP} \right); \tag{1.48}$$

$$\Phi_{TP} = a_{TP} F_{TP} \left(\Theta_C^{CP} - \Theta_{TP}^{CG} \right); \tag{1.49}$$

$$\Phi_{CG} = \frac{F_{CT}^{CP} \left(\Theta_{TP}^{CT} - \Theta_{MTP}^{CT} \right)}{R_T^{\dot{E}}}; \tag{1.50}$$

$$\Theta_C^{CP} - \Theta_{MTP} = \frac{\left(\Theta_{1C} - \Theta_{MTP} \right) - \left(\Theta_{2C} - \Theta_{MTP} \right)}{ln \left[\frac{\Theta_{1C} - \Theta_{MTP}}{\Theta_{2C} - \Theta_{MTP}} \right]}, \tag{1.51}$$

where M_Φ, M_Y^{OUT}, M_X^{IN} – mass flow rate of phlegm, ammonia vapour at the outlet and liquid refrigerant at the inlet, kg/s; i_Φ, i_Y^{OUT}, i_X^{IN} – enthalpy of phlegm, ammonia vapour at the outlet and liquid refrigerant at

the inlet, kJ/kg; ξ_Φ, ξ_Y^{OUT}, ξ_X^{IN} – weight concentration of phlegm, ammonia vapour at the outlet and liquid refrigerant at the inlet, kg/kg; Φ_{CT}, Φ_{MTP}, Φ_{TP} – heat flows through the pipe wall, from the inter-pipe and pipe space, W; F_{CT}^{CP}, F_{MTP}, F_{TP} – surface area of the average wall, inter-pipe and pipe space, m^2; Θ_C^{CP}, Θ_{TP}^{CT}, Θ_{MTP}, Θ_{MTP}^{CT} – average temperature of the heat transfer fluid and the wall on the tube space side, boiling refrigerant and the wall on the intertube space side, °C.

Equations (1.13)–(1.20), (1.40), (1.41), (1.45)–(1.51), together with formulas for calculating the thermophysical properties of substances and equilibrium dependencies, constitute a complete mathematical model of the evaporator. The research was carried out according to the developed algorithm, the software implementation of which was performed in the MATLAB package [26]. A generalised block diagram of the algorithm is shown in **Fig. 1.7**.

The symbols shown in **Fig. 1.7** correspond to the following physical quantities: V_C – volumetric flow rate of the heat transfer medium, nm^3/s; a_i^{IN} – volumetric concentration of the heat transfer medium components at the inlet, % vol., F = 520 m^2 – total heat exchange surface area; ε = 0.2% – specified calculation error value; $\Delta\Theta = 0.1$°C – temperature change step; Θ_C^{CP} – average refrigerant temperature, °C; $\Delta\Theta^{CP}$ – average logarithmic temperature difference, °C; q_{TP}, q_{MTP} – specific heat flux from the pipe and inter-pipe space, W/m^2; M_{KC}, M_Y^{OUT}, M_X^{IN} – average flow rate of condensed ammonia from the central heating system, refrigerant vapour at the evaporator outlet and liquid refrigerant to the condenser receiver, kg/s; r^{CP} – average heat of condensation of ammonia, kJ/kg; a_{TP}, a_{MTP}, K – heat transfer coefficients from the CH, refrigerant and total heat transfer coefficient, W/(m^2·K); R_T^E – total thermal resistance, (m^2·K)/W; P_C, P_{MTP} – pressure of the central heating system and boiling refrigerant, respectively, MPa; ξ_Φ – weight concentration of phlegm, kg/kg; Θ_{MTP} – boiling temperature of the refrigerant in the intertube space, °C; i_X^{IN}, i_Φ, i_Y^{OUT} – enthalpy of the liquid refrigerant at the inlet, phlegm and ammonia vapour at the outlet, kJ/kg; F_X – effective heat exchange surface, m^2; n = 526 – total number of heat exchange tubes; Φ_{TP}, Φ_{MTP} – heat flow from the pipe and inter-pipe space, respectively, MW. Unlike commonly known algorithms, the developed algorithm allows calculating the effective heat exchange surface F_X of the evaporator under external disturbances using the following formula

$$F_X = \Phi / q. \tag{1.52}$$

The algorithm consists of two main convergence cycles. In the first cycle, the temperature Θ_{2C} is determined and the calculation error δ_1 is estimated under the condition $\Delta M_X^{IN} \geq 0$, when the refrigerant and phlegm flow rates do not exceed the possible inflow of liquid refrigerant to the evaporator from the ARU condenser. The second cycle is related to determining the temperature Θ_{2C} and the effective heat exchange surface in the case $\Delta M_X^{IN} < 0$, i.e. under the conditions of the existing restriction on the consumption of liquid refrigerant from the ARU condenser. At the same time, in both cycles, with a constant level, the overall balance of the evaporator in terms of consumption and energy is maintained.

The applicability of the obtained LTE model is confirmed by the calculation results obtained and presented in **Table 1.8**. A comparison of the experimental data given in **Tables 1.1** and **1.2** and the results obtained in **Table 1.8** using the mathematical model shows that the calculation error does not exceed the

approximation error R_T^E according to equation (1.40). At the same time, the root mean square deviation of the calculated values of Θ_{2C} from the experimental values does not exceed 0.17°C.

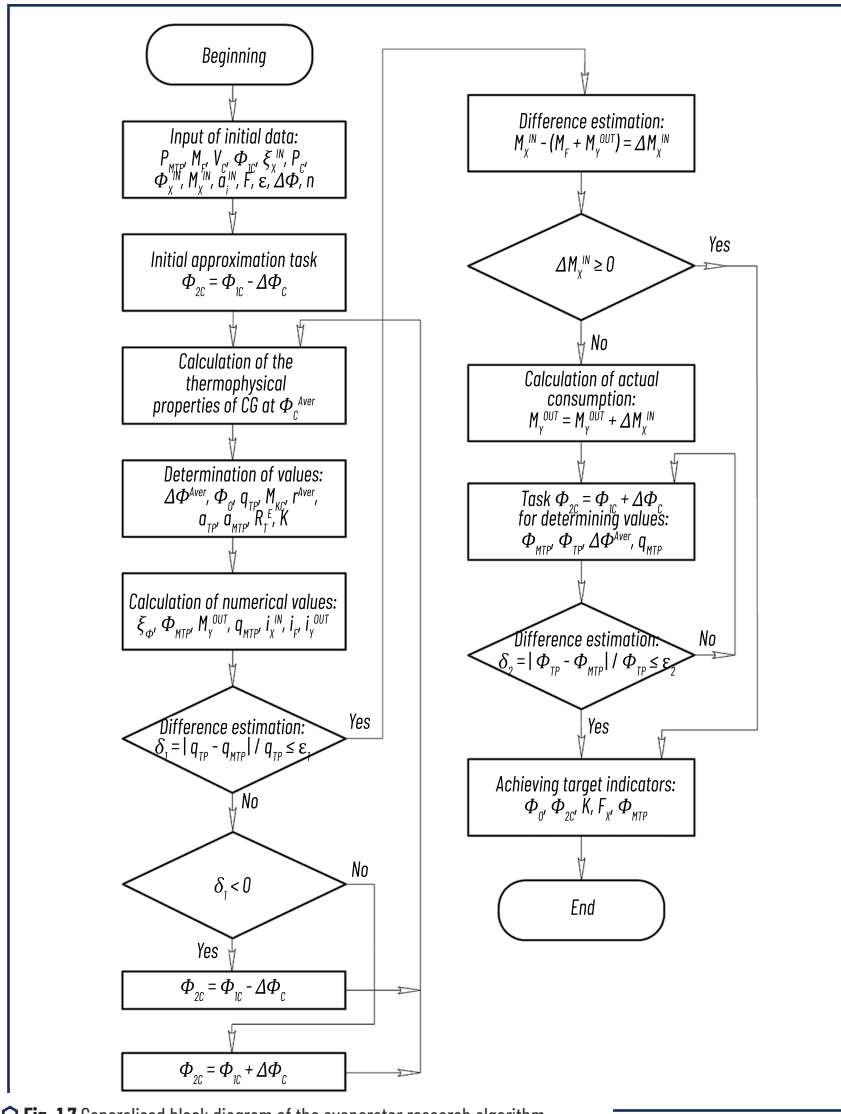

Fig. 1.7 Generalised block diagram of the evaporator research algorithm
Source: [26]

Table 1.8 Calculated indicators of the evaporator operating modes ARU

Indicator name	Mode numbers*						
	1	2	3	4	5	6	7
Ammonia concentration at the inlet $a^{IN}_{NH_3}$, % vol.	9.67	10.15	9.66	9.84	9.14	9.54	8.1
Cooling capacity Φ_0, MW	4.6	5.56	5.04	5.2	3.31	3.26	5.02
Heat transfer coefficient K, W/(m^2·K)	576.05	629.04	579.74	603.54	541.19	544.47	681.67
Boiling point of refrigerant Θ_{MTR}, °C	−14.35	−10.09	−16.51	−14.08	−8.06	−2.87	−16.67
Central heating outlet temperature Θ_{2C}, °C	−4.8	−1.32	−7.57	−5.89	−2.39	4.03	−4.8
Total thermal resistance $R^E_T \cdot 10^4$, (m^2·K)/W	7.125	6.812	7.412	6.941	5.831	6.058	4.746

*Note: *mode numbers correspond to the numbers in **Tables 1.1** and **1.2***
Source: [19]

Mathematical modelling allows us to establish the patterns of influence of variables, both the vector of external disturbances *Z(t)* and the vector of controls *Y(t)*, on the state vector *X(t)* of the evaporator. Moving to the state variable space, these vectors will have the following form:

$$X(t)=\begin{bmatrix}\Theta_{2C}(t)\\ H(t)\end{bmatrix};\quad Z(t)=\begin{bmatrix}\Theta_{1C}(t)\\ a^{IN}_{NH_3}(t)\\ \Theta^{IN}_{X}(t)\\ \xi^{IN}_{X}(t)\\ P_{MTP}(t)\\ V_C(t)\end{bmatrix};\quad Y(t)=\begin{bmatrix}M^{IN}_{X}(t)\\ M_{\Phi}(t)\end{bmatrix}. \tag{1.53}$$

It should be noted that the limitations in the research are due to the range of coordinate changes in the process of developing a mathematical model of the evaporator. The temperature value Θ_{1C} was a constant at 9.2°C, which is ensured by the new technological design of the TCSC.

Fig. 1.8 shows individual research results on the control effect of phlegm flow M_F at different pressures P_{MTP} on the efficiency of the cooling process of the central heating system in the evaporator of the high-pressure turbine under the following restrictions: V_C = 310798 nm^3/s; $a^{IN}_{NH_3}$ = 0.103% vol; $a^{IN}_{H_2}$ = 0.544% vol; $a^{IN}_{N_2}$ = 0.195% vol; $a^{IN}_{CH_4}$ = 0.082% vol; a^{IN}_{Ar} = 0.076% vol; Θ_{1C} = 9.2°C; P_C = 23 MPa; M^{IN}_X = 10 t/h; ξ^{IN}_X = 0.998 kg/kg; Θ^{IN}_X = 26°C.

Fig. 1.9–1.11 show the results of studies on the effect of the control action of the phlegm flow rate M_F on the target indicators of evaporator efficiency, namely the cooling temperature of the refrigerant Θ_{2C} and the cooling capacity of the ARU F_0 under conditions of changing disturbance vector coordinates and under

the above-mentioned restrictions. These are primarily the refrigerant concentration ξ_X^{IN}, the refrigerant flow rate M_X^{IN}, coming from the condenser, and the ammonia concentration in the refrigerant $a_{NH_3}^{IN}$ at the evaporator inlet.

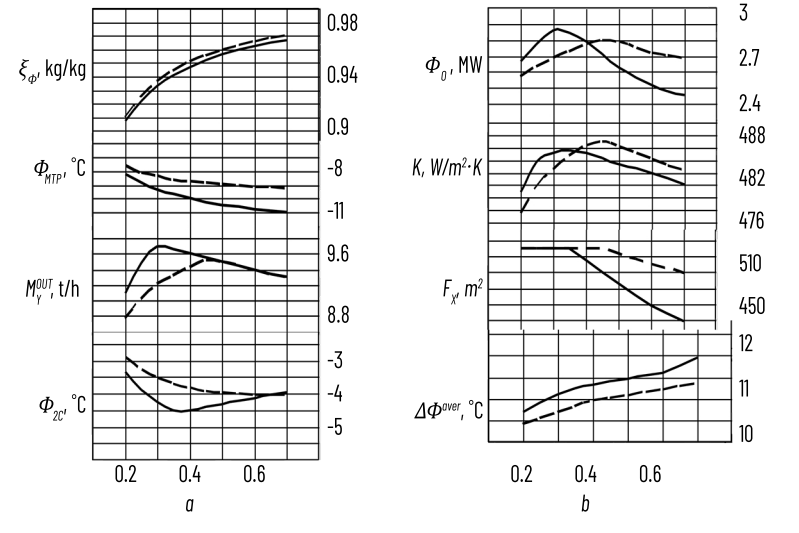

Fig. 1.8 Dependence of the efficiency indicators of the ARU evaporator on the change in pressure P_{MTP} (– – – – P_{MTP} = 0.29 MPa; - - - - - P_{MTP} = 0.3 MPa) and the control action of the phlegm flow rate M_F: *a* — phlegm concentration ξ_Φ, refrigerant boiling temperature in the intertube space Φ_{MTP}, refrigerant vapour flow rate at the evaporator outlet cooling temperature CG Φ_{2C}; *b* — cooling capacity Φ_0, heat transfer coefficient *K*, effective heat exchange surface F_X, mean logarithmic temperature difference $\Delta\Phi^{CP}$
Source: [26]

The dependencies obtained as a result of the research, shown in **Fig. 1.8** for such indicators as cooling capacity Φ_0 and cooling temperature CG Θ_{2C}, are extreme in nature from the control action of the phlegm flow rate M_Φ. This is due, in turn, to the extreme dependence of the refrigerant vapour flow rate M_Y^{OUT}, which increases due to a decrease in the boiling point of the liquid refrigerant Θ_{MTP}. The latter contributes to a decrease in the cooling temperature of the cooling circuit and an increase in cooling capacity.

The values of these coordinates were selected at the levels most characteristic of the summer and winter seasons of operation of the secondary condensation unit, including the ARU.

For example, with an increase in M_F from 0.2 t/h to 0.35 t/h at a constant boiling pressure P_{MTP} = 29 MPa, the average concentration of boiling refrigerant ξ_Φ increases from 0.9071 kg/kg to 0.9408 kg/kg. This, in turn, leads to a decrease in the boiling temperature of the refrigerant Θ_{MTP} from –8.24°C to –9.71°C.

This results in an increase in the average temperature difference of $\Delta\Theta^{CP}$ from 10.68°C to 11.24°C and the consumption of evaporating refrigerant M_Y^{OUT}, from 9.08 t/h to a maximum of 9.65 t/h. Under these circumstances, the temperature Θ_{2C} decreases from –3.36°C to a minimum of –4.5°C, and the cooling capacity Φ_0 increases from 2.66 MW to a maximum of 2.84 MW. The heat transfer coefficient *K* increases and reaches a maximum value of 485.5 W/(m^2·K). This indicates, as is CCown [27], that the critical limit of the bubble boiling regime of the refrigerant has been reached. At the same time, by reducing the temperature of the Θ_{2C} by 1.14°C through the control action on the phlegm flow rate, a reduction in natural gas consumption of 50 thousand nm^3/year is achieved.

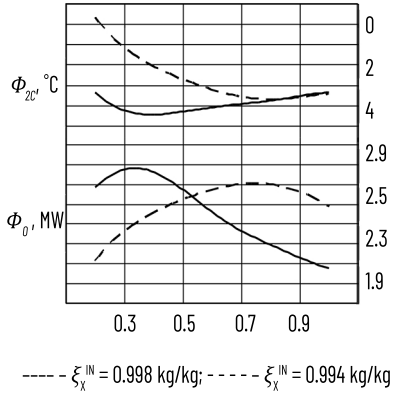

Fig. 1.9 Dependence of the cooling temperature Φ_{2C} and the cooling capacity Φ_0 of the ARU on the control action of the phlegm flow M_Φ at different values of the refrigerant concentration ξ_X^{IN} at the evaporator inlet

A further increase in the control action of M_F, for example to 0.5 t/h, leads to an increase in the concentration of ξ_Φ, a decrease in the temperature of Θ_{MTP} and an increase in the temperature difference $\Delta\Theta^{CP}$ to 0.9562 kg/kg, –10.1°C and 11.32°C, respectively. This reduces the effective heat exchange surface from 520 m^2 to 481.27 m^2 indicating the establishment of a transitional boiling regime for the refrigerant. This mode is characterised by the formation of large vapour cavities on the surface itself. As a result, "dry" areas appear on the surface, which seem to exclude part of the surface from heat exchange. Under such conditions, heat transfer directly to the steam is less intense. This causes a decrease in steam consumption M_Y^{OUT} to 9.52 t/h, heat transfer coefficient K to 482.5 W/(m^2·K), and cooling capacity Φ_0 to 2.63 MW. At the same time, the cooling temperature of the Θ_{2C} will increase to –4.25°C, i.e. by 0.25°C, and the annual consumption of natural gas will increase by almost 77 thousand nm^3.

The increase in pressure is most often caused by an increase in the temperature of the water cooling the absorber. According to **Fig. 1.8**, an increase in pressure P_{MTP} from 0.29 MPa to 0.3 MPa necessitates an increase in the flow rate M_F from 0.35 t/h to 0.45 t/h to establish the critical limit of the bubble boiling regime of the refrigerant. At the same time, due to an increase in the temperature difference $\Delta\Theta^{CP}$ from 10.83°C

to a critical 11.01°C, the cooling capacity will increase from 2.73 MW to a maximum of 2.79 MW, and the cooling temperature of the central heating system Θ_{2C} will decrease from −3.7°C to a minimum of −3.98°C. As a result of this control action on consumption, annual natural gas consumption can be reduced by 88 thousand nm^3/year.

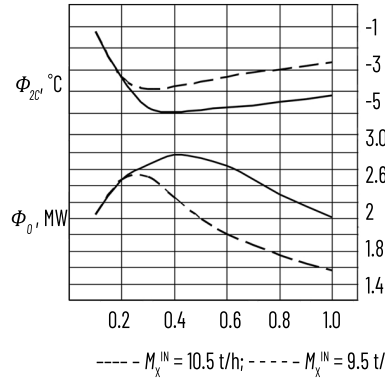

Fig. 1.10 Dependence of the cooling temperature of the central heating system Φ_{2C} and the cooling capacity of the ARU Φ_0 on the control action of the phlegm flow rate M_Φ at different refrigerant flow rate M_X^{IN} at the evaporator inlet
Source: [26]

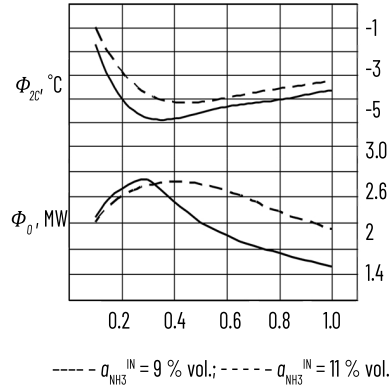

Fig. 1.11 Dependence of the cooling temperature of the central heating system Φ_{2C} and the cooling capacity of the automatic control system Φ_0 on the control action of the phlegm flow rate M_Φ at different values of ammonia concentration in the central heating system Θ_{2C} at the evaporator inlet
Source: [26]

The concentration of liquid refrigerant at the evaporator inlet ξ_X^{IN} also varies within a fairly wide range due to seasonal fluctuations in the air temperature cooling the ARU condenser. As can be seen from **Fig. 1.9**, the extreme (minimum) value of the temperature Θ_{2C} with an increase in the concentration ξ_X^{IN} from 0.994 kg/kg to 0.998 kg/kg decreases from −3.8°C to −4.5°C at a constant pressure P_{MTP} = 0.29 MPa. At the same time, there is a shift towards a decrease in the control action of the phlegm flow rate from 0.8 t/h to 0.35 t/h, at which the minimum values of Θ_{2C} are ensured. Under such conditions, the cooling capacity increases from 2.69 MW to 2.84 MW, and the annual consumption of natural gas can be reduced by 215 thousand nm^3.

With a constant heat supply to the rectifier generator and seasonal fluctuations in condensation pressure, there is also a change in the flow rate of refrigerant vapour entering the condenser and liquid refrigerant entering the evaporator. As a result of these changes in consumption M_X^{IN}, for example, from 9.5 t/h to 10.5 t/h (**Fig. 1.10**), there is also a shift in the required control action of the phlegm consumption from 0.3 t/h to 0.4 t/h, at which the minimum temperature values are achieved Θ_{2C} namely at −3.9°C and −4.98°C. At the same time, the maximum cooling capacities F_0 of 2.71 MW and 2.96 MW, respectively, are ensured. Due to such control action on the phlegm flow rate, the annual natural gas consumption is reduced by 332 thousand nm^3.

The concentration of ammonia in the central heating system changes significantly as a result of the use of air cooling at the primary condensation stage $a_{NH_3}^{IN}$, which causes a change in the heat load of the evaporator. According to the obtained dependencies (**Fig. 1.11**), with a decrease in the concentration of $a_{NH_3}^{IN}$ from 11% vol. to 9% vol., the extreme shifts towards a decrease in the control action of the phlegm consumption, i.e. from 0.4 t/h to 0.3 t/h.

Under these conditions, extreme values of the temperature of the Θ_{2C} are observed at −4.22°C and −4.98°C, respectively, and the cooling capacity reaches maximum values of 2.8 MW and 2.85 MW. At the same time, the annual consumption of natural gas can be reduced by 234 thousand nm^3.

The above studies have proven the significant impact of phlegm consumption for such powerful ARU on the cooling efficiency of the central heating system and, consequently, on the energy efficiency of production. At the same time, the use of control action on phlegm consumption in the range from 0.2 t/h to 0.8 t/h provides a reduction in annual natural gas consumption by an average of 500 thousand nm^3.

The established extreme nature of the dependence of the cooling temperature of the central heating system Θ_{2C} on the control action of the phlegm flow and the shift of the extreme in conditions of changing values of the disturbance vector coordinates *Z(t)* confirms the need to build a system of optimal software control of the cooling temperature regime of the central heating system. The main link in such a system should be an optimisation subsystem for calculating the value of the coordinate of the control action of the phlegm flow rate, which determines the optimal state vector *X(t)* of the evaporator.

Analysis of the above calculation process indicates the possibility of solving a multidimensional optimisation problem using a step-type non-gradient method with one-dimensional extremum search algorithms [28]. Non-gradient methods are, by their nature, most suitable for optimising existing industrial systems. Given the sensitivity of the object to changes in phlegm flow, it is most appropriate to use a scanning method in the space of only one variable. This method guarantees that the extremum will not be missed due

to the use of a small search step [29]. Taking this into account and the dependencies obtained, a search step for phlegm flow rate of 0.02 t/h was adopted. In this case, the block diagram of the algorithm shown in **Fig. 1.7** must be supplemented with a third cycle of searching for a global extremum.

The resulting algorithmic support for minimising the cooling temperature Θ_{2C} of the central heating system allows it to be used in the optimisation subsystem. This subsystem is a key component in the overall technical structure of the computer-integrated system for optimal software control of the ARU evaporator.

1.5 TECHNICAL STRUCTURE OF THE COMPUTER–INTEGRATED SYSTEM FOR OPTIMAL SOFTWARE CONTROL

The TDC-3000 information and control system, which is used in the AM-1360 series ammonia synthesis units operating in Ukraine, covers both the field and technological levels of production control. It includes means for collecting, processing and storing technological information, as well as human-machine interface tools. Information exchange is carried out using communication tools. However, it should be noted that TDC-3000 is a "closed" type control system with pre-installed software. Therefore, it cannot be significantly upgraded. The solution to the task of building a mathematical model in real time and adapting the model to a situation of uncertainty is only possible by supplementing the existing control system with available open-type hardware and software.

Fig. 1.12 shows an option for combining TDC-3000 with the proposed automated system for identification, creation of a mathematical model and minimisation of the temperature regime of the ARU evaporator [19].

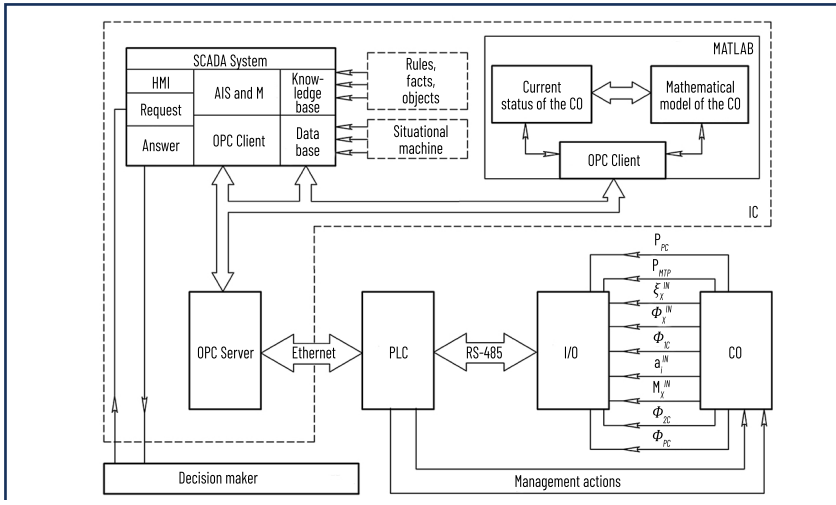

Fig. 1.12 Generalised technical structure of the automated system for optimal software control of the ARU evaporator
Source: [19]

This approach allows the TDC-3000 to be used as a source of operational technological information for filling the database and knowledge base. This is made possible by the use of OPC technology, which allows all the necessary information to be obtained using a client-server method of data access [30]. The SCADA system and the MATLAB software environment perform the client function in the system. With this approach, the SCADA system provides the human-machine interface function, and all the necessary calculations are performed in the MATLAB software environment [31]. As a result, control algorithms can be supplemented with new data regarding the mathematical model, which will ensure the solution of the problem of minimising the temperature regime of the evaporator of the secondary condensation unit in real time.

CONCLUSIONS

Improving the energy efficiency of ammonia production, in particular the secondary condensation process complex (SCPC) as one of the most energy-intensive components, is becoming particularly relevant in the overall process of modernising large-scale synthesis units. The greatest efficiency of modernisation is ensured by the application of a systematic approach through the combination of its systemic-structural and systemic-control positions, the scientific basis of which is mathematical modelling and process identification.

Research has established uncertainties in the operation of the TRU, and algorithms have been developed for forming an information array of experimental data and numerical assessment of uncertainties. The heat exchange processes for the condensation column (CC) and low-temperature evaporators (LTE) included in the TCSC, based on which equations were determined for calculating the heat transfer coefficients, heat transfer and ammonia concentration in the circulating gas at the outlet of the separation part of the CC. It has been shown that, unlike the well-known equations, these equations take into account the condensation thermal resistance in the heat exchange process and the external material and thermal load on the CC. The synthesis of the instrumental and technological design of the TCSC was carried out only with the use of heat-using absorption-refrigeration and steam ejector units, the operation of which is ensured by the utilisation of low (up to 150°C) and ultra-low (up to 90°C) temperature potential of the heat of material flows of the ammonia synthesis unit. The efficiency indicators for the created optimal structure of the TCSC in terms of reducing the total cooling capacity, specific energy consumption of electricity and natural gas, which are 2.66 MW, 60 kW·h/t NH^3 and 1.2 m^3/t NH^3, respectively, have been determined.

Based on the results of mathematical modelling, the dependencies of the evaporator heat exchange efficiency indicators on changes in the phlegm flow control action and the coordinates of the external disturbance vector have been determined. Among these indicators, the following should be highlighted: heat flows, cooling capacity, cooling temperature of the central heating system, temperature head, and heat transfer coefficients. A pattern of extreme dependence of cooling capacity and cooling temperature of the refrigerant on the phlegm flow rate has been established, an increase in which leads to an increase in the temperature head of the evaporator. Achieving maximum cooling capacity, and therefore minimum cooling temperature of the central heating system at a certain temperature head, is determined by the critical regime of bubble boiling of the refrigerant. A further increase in temperature head with an increase in phlegm

flow contributes to the establishment of a transitional boiling regime. This regime is characterised by the appearance of "dry" areas on the heating surface, which leads to a decrease in the effective heat exchange surface, cooling capacity and an increase in the cooling temperature of the central heating system. The obtained dependencies of the cooling temperature of the refrigerant on the control action of the phlegm flow rate characterise the shift of the extreme under conditions of changing values of the disturbance vector coordinates, and, consequently, the change in the energy efficiency indicators of ammonia production (annual natural gas consumption) when changing the disturbance vector coordinates.

Algorithmic support has been developed to solve the problems of identification, obtaining a mathematical model of the HTV evaporator and numerical estimation of the optimal state vector (cooling temperature of the central heating system). The use of the algorithm implemented in the MATLAB package provides a real-time solution to the optimisation problem using a step-type non-gradient method with the application of one-dimensional extremum search methods. The technical structure of a computer-integrated system for optimal software control of the temperature regime of a low-temperature evaporator has been determined, which is adapted to the existing information system of an industrial ammonia synthesis unit.

The scientific results obtained develop the field of knowledge on the creation of energy-efficient technological cooling systems through the utilisation of heat with ultra-low temperature potential and adaptive systems for optimal software control under uncertainty.

REFERENCES

1. Heidlage, M., Pfromm, P. H. (2015). Novel Thermochemical Synthesis of Ammonia and Syngas from Natural Gas. 2015 AIChE Annual Meeting Proceedings, 517b. Available at: https://proceedings.aiche.org/conferences/aiche-annual-meeting/2015/proceeding/paper/517b-novel-thermochemical-synthesis-ammonia-and-syngas-natural-gas
2. Dawson, C. J., Hilton, J. (2011). Fertiliser availability in a resource-limited world: Production and recycling of nitrogen and phosphorus. Food Policy, 36 (1), 14–22. https://doi.org/10.1016/j.foodpol.2010.11.012
3. Dybkjær, I. (2013). 100 Years of Ammonia Synthesis Technology. Ammonia Technical Manual, 101–109. Available at: https://www.scribd.com/document/478848969/011
4. Noelker, D. K., Ruether, J. (2011). Low Energy Consumption Ammonia Production: Baseline Energy Consumption, Options for Energy Optimization. Nitrogen + Syngas Conference 2011, Duesseldorf 14.
5. Singh, U., Singh, S., Malhotra, A. (2010). Successful Operating Experience of CFCL Ammonia Plant Revamped with KBR KRES Technology. Ammonia plant safety (and related facilities). Safety in ammonia plants & related facilities symposium, 121–130.
6. Rouwenhorst, K. (2024). Technology options for low-emission ammonia production from gas. Ammonia Energy Association. Available at: https://ammoniaenergy.org/articles/technology-options-for-low-emission-ammonia-production-from-gas/
7. Mishra, R. S., Dwivedi, A., Ahmad, S. (2017). A thermodynamic analysis of ejector type vapour refrigeration system using eco-friendly refrigerants. International Journal of Research in Engineering and

Innovation, 1 (2), 40–48. Available at: https://ijrei.com/assets/frontend/aviation/[6]%20IJREI_vol-1,%20Issue-2.pdf

8. Babichenko, A. K., Toshynskyi, V. I. (2009). Zastosuvannia matematychnoho modeliuvannia dlia diahnostyky pokaznykiv efektyvnosti protsesiv teplo-i masoobminu v absorberakh teplovykorystuiuchykh kholodylnykh ustanovok ahrehativ syntezu amiaku. Voprosy khymyy y khymycheskoi tekhnolohyy, 6, 107–111.
9. Ladaniuk, A. P. (2015). Suchasni metody avtomatyzatsii tekhnolohichnykh obiektiv. Intehral Lohistyk Ukraina, 408.
10. Wu, H., Wang, W., Ye, H. (2015). Robust state estimation for linear systems with parametric uncertainties and quantised measurements. International Journal of Systems Science, 46 (3), 526–534. https://doi.org/10.1080/00207721.2013.807387
11. Fronk, B. M., Garimella, S. (2016). Condensation of ammonia and high-temperature-glide ammonia/water zeotropic mixtures in minichannels – Part I: Measurements. International Journal of Heat and Mass Transfer, 101, 1343–1356. https://doi.org/10.1016/j.ijheatmasstransfer.2016.05.049
12. Malyshev, V. V., Krietov, V. V., Hladka, T. M. Tekhnichna termodynamika ta teploperedacha. Universytet "Ukraina", 257.
13. Chen H. F., Zhang J.-F. (1990). Stochastic Adaptive Control for ARMAX Systems with Unknown Orders, Time-Delay and Coefficients. IFAC Proceedings Volumes, 23 (8 (2)), 267–272. https://doi.org/10.1016/S1474-6670(17)52019-4
14. Ladaniuk, A. P., Reshetiuk, V. M., Kyshenko, V. D., Smitiukh, Ya. V. (2014). Innovatsiini tekhnolohii v upravlinni skladnymy biotekhnolohichnymy obiektamy ahropromyslovoho kompleksu. Tsentr uchbovoi literatury, 280.
15. Brandt, S. (2014). Data Analysis: Statistical and Computational Methods for Scientists and Engineers. Springer, 523.
16. Babichenko, A., Velma, V., Babichenko, J., Kravchenko, Y., Krasnikov, I. (2017). System analysis of the secondary condensation unit in the context of improving energy efficiency of ammonia production. Eastern-European Journal of Enterprise Technologies, 2 (6 (86)), 18–26. https://doi.org/10.15587/1729-4061.2017.96464
17. Babichenko, A. K., Podustov, M. O., Kravchenko, Y. O., Babichenko, Y. A. (2019). Formation of the information array of the identifier of the adaptive control system of the ammonia production condensation unit with uncertainties. Bulletin of the National Technical University "KhPI" A series of "Information and Modeling", 13 (1338), 24–32. Available at: http://pim.khpi.edu.ua/article/view/2411-0558.2019.13.03
18. Mendenhall, W., Sincich, T. (2002). A Second Course in Statistics: Regression Analysis. Prentice Hall, 880.
19. Babichenko, A., Babichenko, J., Kravchenko, Y., Velma, S., Krasnikov, I., Lysachenko, I. (2018). Identification of heat exchange process in the evaporators of absorption refrigerating units under conditions of uncertainty. Eastern-European Journal of Enterprise Technologies, 1 (2 (91)), 21–29. https://doi.org/10.15587/1729-4061.2018.121711
20. Babichenko, A. K. (2010). Zakonomirnosti teploobminu v protsesi kondensatsii amiaku z tsyrkuliatsionoho hazu u vyparnykakh ahrehativ syntezu. Intehrovani tekhnolohii ta enerhozberezhennia, 1, 47–51.

21. Babichenko, A. K., Podustov, M. O., Kravchenko, Ya. O. (2018). Systemnyi pidkhid shchodo stvorennia optymalnoi struktury ta systemy upravlinnia tekhnolohichnoho kompleksu vtorynnoi kondensatsii vyrobnytstva amiaku. Proceedings of the 8th International Conference Science and society, 145—-155.
22. Babichenko, A. K., Toshynskii, V. I., Krasnikov, I. L., Podustov, M. A. (2007). Enerhosberehaiushchee tekhnolohycheskoe oformlenye bloka vtorychnoi kondensatsyy krupnotonnazhnykh ahrehatoa synteza ammyaka. Intehrovani tekhnolohii ta enerhozberezhennia, 4, 3—6.
23. Garimella, S., Mostafa, S., Sheldon, M. (2012). Ammonia-water desorption in flooded columns. Georgia Institute of Technology, 148.
24. Shukla, A., Mishra, A., Shukla, D., 4Karan Chauhan, K. (2015). C.O.P derivation and thermodynamic calculation of ammonia-water vapor absorption refrigeration system. International Journal of Mechanical Engineering and Technology, 6 (5), 72—81. Available at: https://iaeme.com/MasterAdmin/Journal_uploads/IJMET/VOLUME_6_ISSUE_5/IJMET_06_05_010.pdf
25. Lutska, N. M., Ladaniuk, A. P. (2016). Optymalni ta robastni systemy keruvannia tekhnolohichnymy obiektamy. Lira-K, 288.
26. Babichenko, A., Kravchenko, Y., Babichenko, J., Krasnikov, I., Lysachenko, I., Velma, V. (2018). Algorithmic tools for optimizing the temperature regime of evaporator at absorption-refrigeration units of ammonia production. Eastern-European Journal of Enterprise Technologies, 4 (2 (94)), 29—35. https://doi.org/10.15587/1729-4061.2018.139633
27. Çengel, Y. A. (2007). Introduction to Thermodynamics and Heat Transfer. McGraw-Hill, 922.
28. Hare, W., Nutini, J., Tesfamariam, S. (2013). A survey of non-gradient optimization methods in structural engineering. Advances in Engineering Software, 59, 19—28. https://doi.org/10.1016/j.advengsoft.2013.03.001
29. Ravindran, A., Ragsdell, K. M., Reklaitis, G. V. (2006). Engineering Optimization: Methods and Applications. John Wiley & Sons, 667. https://doi.10.1002/9780470117811
30. Sharma, K. L. S. (2016). Overview of industrial process automation. Elsevier, 492.
31. Pacaux-Lemoine, M.-P., Trentesaux, D., Zambrano Rey, G., Millot. P. (2017). Designing intelligent manufacturing systems through Human-Machine Cooperation principles: A human-centered approach. Computers & Industrial Engineering, 111, 581—595. https://doi.10.1016/j.cie.2017.05.0201814